Ultrasound in Med. & Biol., Vol. 42, No. 1, pp. 1–15, 2016

0301-5629/$ - see front matter

http://dx.doi.org/10.1016/j.ultrasmedbio.2015.08.016

● *Review*

BIOLOGICAL EFFECTS OF LOW-FREQUENCY SHEAR STRAIN: PHYSICAL DESCRIPTORS

Edwin L. Carstensen,*† Kevin J. Parker,*† Diane Dalecki,*† and Denise C. Hocking†‡

*Department of Electrical & Computer Engineering, University of Rochester, Rochester, New York, USA; †Department of Biomedical Engineering, University of Rochester, Rochester, New York, USA; and ‡Department of Pharmacology and Physiology, University of Rochester Medical Center, Rochester, New York, USA

(*Received* 1 *May* 2015; *revised* 24 *August* 2015; *in final form* 24 *August* 2015)

Abstract—Biological effects of megahertz-frequency diagnostic ultrasound are thoroughly monitored by professional societies throughout the world. A corresponding, thorough, quantitative evaluation of the archival literature on the biological effects of low-frequency vibration is needed. Biological effects, of course, are related directly to what those exposures do physically to the tissue—specifically, to the shear strains that those sources produce in the tissues. Instead of the simple compressional strains produced by diagnostic ultrasound, realistic sources of low-frequency vibration produce both fast (∼1,500 m/s) and slow (1–10 m/s) waves, each of which may have longitudinal and transverse shear components. Part 1 of this series illustrates the resulting strains, starting with those produced by longitudinally and transversely oscillating planes, through monopole and dipole sources of fast waves and, finally, to the case of a sphere moving in translation—the simplest model of the fields produced by realistic sources. (E-mail: ecarsten@rochester.rr.com) **© 2016 World Federation for Ultrasound in Medicine & Biology.**

Key Words: **Biological effects, Low-frequency vibration, Low-frequency shear strain, Acoustic monopole, Acoustic dipole, Tactile perception, Transverse and longitudinal shear waves.**

INTRODUCTION

Years before ultrasound became a useful diagnostic tool, it was well established as a form of diathermy because it could generate heat deep within tissues. Now that ultrasound has become one of medicine's most valuable imaging systems, our professional organizations periodically review bio-effects research and formulate guidelines for safe use of diagnostic equipment. Those guidelines usually are expressed in the language of machine output (thermal or mechanical indices) or as estimated acoustic pressures in the tissues. Those are quantities that are under direct control of the operator.

Biological effects, of course, are related directly to what those exposures do physically to the tissue. Consider the effects of tissue exposed to ultrasound first in its normal state and then after infusion with contrast microbubbles. In their normal state, most tissues are undamaged by the highest exposures permitted under Food and Drug Administration guidelines (FDA 1993). With bubbles present, however, significant microvascular damage may occur at those exposure levels. The explanation, of course, is that tissue shear strains near oscillating bubbles are many orders of magnitude greater than strains in tissue exposed to the same acoustic stresses but in the absence of those bubbles (Carstensen et al. 2011).

Sound, ultrasound, vibration and the waves associated with these phenomena all involve time-dependent displacements of the particles that constitute the exposed media. When a particle and its neighbors all move together, we have rigid displacement. It is unlikely that simply moving the medium, unchanged, from one place to another will cause a biological effect. Even when the force densities associated with acceleration are large, it is more likely that associated bio-effects are directly related to the resulting mechanical changes (strains) in the tissue than to the forces that cause those changes. For that information, we turn to the gradient of the displacement, the space rate of change of the displacement, which tells us how an element of the tissue has been changed in size, shape and rotation.

Although there has been no direct test of the hypothesis, rigid rotation, the asymmetric part of the

Address correspondence to: Edwin L. Carstensen, 103 Eastland Avenue, Rochester, NY 14618-1027, USA. E-mail: ecarsten@rochester.rr.com

displacement gradient, like rigid displacement, seems unlikely to be responsible for biological effects. That leaves us with strain, the symmetric part of the displacement gradient. Strain involves changes in volume (bulk strain) and changes in shape (shear strain). With realistic sources of low-frequency vibration, shear strains are orders of magnitude greater than bulk strain as shown below. That leaves us with shear strain as the chief suspect in the observed biological effects of low-frequency vibration.

At present, no consensus group has undertaken a systematic evaluation of the biological effects of low-frequency strains. This and subsequent sections of this study are aimed at filling that gap temporarily and perhaps providing a starting point for future consensus groups dedicated to periodic reviews in the manner of the bio-effects groups of the World Federation of Ultrasound in Medicine (WFUMB) and the American Institute of Ultrasound in Medicine (AIUM), among others. This document is concerned primarily with physical phenomena and concludes with brief examples from the well-established field of tactile perception. Critical reviews of the archival literature on wound and bone healing are to follow.

Thanks to developments in the field of elastography over the last two decades, we now have the tools needed to measure low-frequency strains in tissues directly. The primary parameters, particle displacement and particle velocity, are currently measured with sub-micrometer sensitivity. Some forms of quantitative elastography that are currently practiced compute shear strain from the space rate of change of the measured displacements. Low-frequency shear strain, however, is not a single number. It remains for some standards group to find a simple, yet informative quantity or quantities for use as exposure parameters in biological effects studies. Despite the fundamental importance of strain in bio-effects, no bio-effects investigators to our knowledge have taken advantage of these techniques. In fact, strain is rarely mentioned in the bio-effects literature.

FIELDS OF VIBRATION SOURCES: IDEALIZED PLANE WAVES

The fields of all vibration sources are oscillating displacements of the particles that make up the medium to which the sources are coupled. For a broader understanding of these fields, let us make the trip to realistic, low-frequency, shear strain fields in four steps (Fig. 1): (i) idealized plane waves; (ii) waves generated by the breathing modes of spherical sources; (iii) acoustic dipoles, two breathing mode spherical sources expanding and contracting out of phase; (iv) waves generated by a rigid sphere moving in translation.

In the real world, we do not have the infinite plane waves that are idealized in acoustics, but some cases are close enough that a plane wave can serve as a useful approximation, for example, very close to a finite, plane source or at the small region in a focused wave where the transition from converging to diverging fields takes place. The primary value of the plane wave concept is its simplicity.

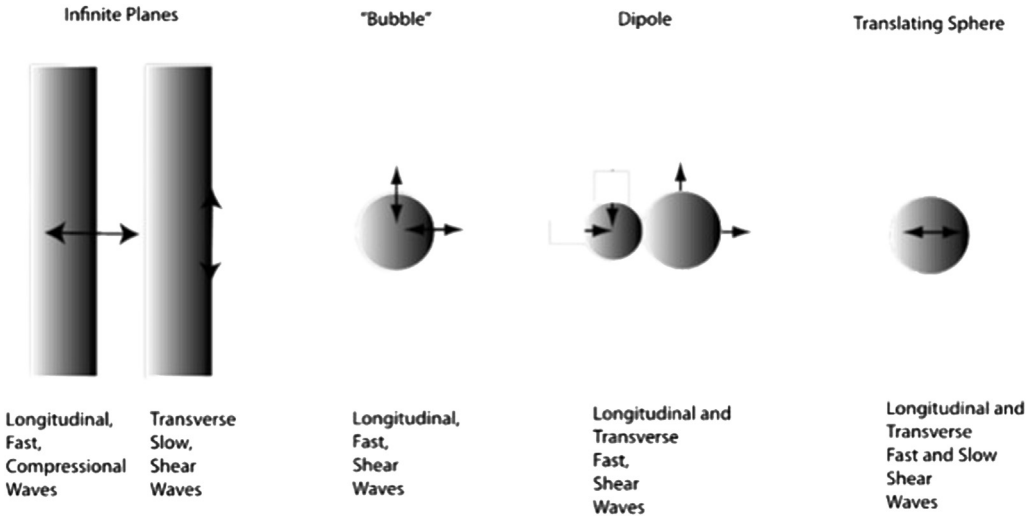

Fig. 1. Realistic sources of low-frequency vibration produce complex combinations of longitudinal and transverse, fast and slow waves in tissues. A sphere moving in translation produces all such fields. To help put these complex fields in perspective with simpler, more frequently studied examples, the discussion moves from plane waves through simple spherical fast waves ("Bubble"), fast dipole spherical waves (from two spherical sources with opposing phases), to the case of the translating sphere. *Arrows* indicate direction of motion of the source.

With an infinite piston as the source, all particle displacement is longitudinal, that is, along the direction of propagation. The wave speed is

$$c_f = \sqrt{\frac{\kappa + \frac{4}{3}\mu}{\rho}}$$

where κ is the bulk modulus, μ is the shear modulus and ρ is density. In principle, both moduli may be complex numbers, which would make the wave speed and propagation constant,

$$k = \beta_f - j\alpha_f = \frac{\omega}{c_f}$$

complex, where

$$\beta_f = \frac{\omega}{c_{f\phi}} = \frac{2\pi}{\lambda_f},\ j = \sqrt{-1},$$

α_f is the absorption coefficient, and ω is the angular frequency (Carstensen and Parker 2014). The phase velocity of the fast wave, $c_{f\phi} = \omega/\beta_f$, is the speed needed to stay at the peak of the fast wave as it moves through the propagating medium. It is a real number on the order of 1,500 m/s in most soft tissues. The wavelength λ_f is also a real number. "Low frequency" for the purpose of these reviews is that for which shear strain dominates. As illustrated in later figures (Figs. 5 and 9), the transition between dominance by shear and dominance by compression is on the order of 20 kHz for sources of interest.

With our best estimates of the stiffness and viscosity of tissues, the simple viscoelastic model predicts that the real bulk modulus dominates c_f for longitudinal plane waves up to frequencies on the order of 1 GHz. So, for tissues at low frequencies, c_f would be almost completely real (the absorption coefficient is effectively zero). (This statement ignores what we know about macromolecular contributions to absorption; however, even those losses in the fast waves are negligible at audio frequencies.)

For the longitudinal, plane wave, the displacement is

$$\vec{\xi}(x,t) = \xi_0 e^{j(\omega t - kx)} \vec{e}_x \tag{1}$$

where $\vec{e}_x$ is the unit vector in the x-direction, and the displacement gradient and strain are

$$\nabla \vec{\xi}(x,t) = \vec{\vec{S}} = \xi_0 e^{j(\omega t - kx)} \begin{bmatrix} -jk & 0 & 0 \\ 0 & 0 & 0 \\ 0 & 0 & 0 \end{bmatrix} \tag{2}$$

The gradient of a vector quantity is just the package of the gradients of each of the scalar components of the vector, making it a second-order tensor. In this case, the gradient is identical to the strain, and for a plane longitudinal wave, it is entirely bulk strain. Because the hypothetical plane wave is attenuated neither by absorption nor by geometric factors, the strain depends only on the spatial change of displacement in the wave. As indicated by eqn (2), this bulk strain is proportional to the propagation constant k, which is very much less than unity at the frequencies of interest. The shapes of elements of the medium change. However, this shape change does not qualify as shear strain because it is a volume change. By definition, shear strain does not involve compression or dilatation, and bulk strain is irrotational.

In contrast to the fast, longitudinal plane wave, when the source plane vibrates in a direction normal to the direction of propagation, we get pure, slow, transverse waves. The strain is entirely shear, and the elements of the medium are rotated. For a given source amplitude, the transverse strains are frequently orders of magnitude greater than the longitudinal strains.

$$\vec{\xi}(x,t) = \xi_0 e^{j(\omega t - hx)} \vec{e}_y \tag{3}$$

where $h = \omega/c_s$, $c_s = \sqrt{\mu/\rho}$,

$$\nabla \vec{\xi} = \xi_0 e^{j(\omega t - kx)} \begin{bmatrix} 0 & 0 & 0 \\ -jh & 0 & 0 \\ 0 & 0 & 0 \end{bmatrix} \tag{4}$$

$$\vec{\vec{S}} = \xi_0 e^{j(\omega t - kx)} \begin{bmatrix} 0 & \frac{-jh}{2} & 0 \\ \frac{-jh}{2} & 0 & 0 \\ 0 & 0 & 0 \end{bmatrix} \tag{5}$$

and

$$\vec{\vec{R}} = \xi_0 e^{j(\omega t - kx)} \begin{bmatrix} 0 & \frac{jh}{2} & 0 \\ \frac{-jh}{2} & 0 & 0 \\ 0 & 0 & 0 \end{bmatrix} \tag{6}$$

where $\vec{\vec{R}}$ is the rotation.

The real and imaginary parts of the shear modulus for tissues are comparable in magnitude at frequencies on the order of ω = 1,000/s (~150 Hz). Thus, in contrast to the longitudinal fast wave, the absorption coefficient for the transverse, slow wave has a strong effect on both displacement and strain.

In summary, the plane wave model gives us two conceptually different waves. One is longitudinal and fast (~1,500 m/s for tissue). The strains that it produces involve compression and dilatation and, therefore,

qualify as bulk strains rather than shear strains. There is no particle rotation. The other wave is transverse and much slower than the longitudinal wave (between 1 and 10 m/s for soft tissues). The wave distorts the tissue in two ways. Elements of the medium change shape (transverse, shear strain), and they are rotated. Furthermore, the shear strains are orders of magnitude greater than the bulk strain for a given applied stress. With idealized plane waves, the strains are either longitudinal and fast or transverse and slow.

This may be a good point in the discussion to pause and ask ourselves what eqns (1)–(6) are telling us about the real, physical processes that take place in the propagating medium and that are important for biological effects. First, simplify the question by assuming that the single-frequency, sinusoidal source has been active long enough for conditions to have reached a steady state. It turns out that in the steady state, some trigonometric computations can be made easier by using Euler's relationship and converting the real expressions into exponentials. For example, eqn (3) is

this oscillation relative to the source is important for biological effects. For those reasons, much of the information that follows is limited to the amplitude or absolute magnitude of the strain with the understanding that it is just a cap on the wave that moves as a sinusoid through the medium.

When the transverse sinusoidal displacement of the source is $\xi_0 \cos(\omega t)\vec{e_y}$, the displacement in the medium at x is $\xi_0 e^{-\alpha x} \cos(\omega t - \beta x)\vec{e_y}$ Using parameters that are representative of soft tissues ($\mu_1 = 1\ kPa$, $\mu_1 = 3\ Pa\ s$), Figure 2 gives the amplitude (absolute magnitude) and a snapshot of the instantaneous values of the displacement at $t = 0$ as given by eqn (3). If we pick any point along the x-axis and observe the displacement with the passage of time, the particle will oscillate normal to the direction of propagation at 1,000 rad/s (~160 Hz) with an amplitude given by the *dashed line*. It lags behind the source and has smaller amplitude than the source because of absorption and geometric spreading.

While eqns (1) and (3) describe the displacement of particles in the propagating medium, eqns (2) and (4) are

$$\vec{\xi}(x,t) = \xi_0 e^{-\alpha x} \cos(\omega t - \beta x)\vec{e_y} = \mathrm{Re}\left[\xi_0 e^{-\alpha x} e^{j(\omega t - \beta x)}\right]\vec{e_y} = \mathrm{Re}\left[\xi_0 e^{j(\omega t - hx)}\right]\vec{e_y} \tag{7}$$

This practice is so common that eqns (1)–(6) use that tool without apology. We can continue our computations of strain this way with the understanding that only the real parts of our solutions have physical meaning. But it is the real magnitude and phase of the whole expression that have meaning, not individual real or imaginary components within it.

The magnitudes of the strains and the frequency at which the strain oscillates at those magnitudes tell almost the whole story. It is unlikely that the phase of

descriptions of the change in relationship of particles to their neighbors. If instead of a single particle we observe a small collection of particles in the form of a square at a distance x from the source, eqn (5) and Figure 3 tell us that the diagonals of that square will be sinusoidally stretched and shrunk in such a way that the area of the square remains constant.

Rotation may not play an important role in bioeffects, but it is involved in all slow, transverse waves. The rotation of the elemental square is equal in

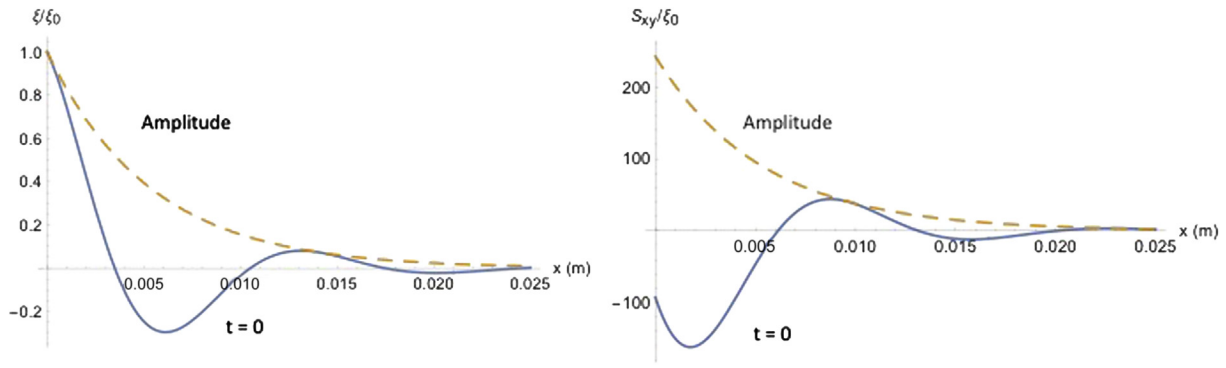

Fig. 2. Displacements (left) and strains (right) given by eqns (3) and (5). $\mu = \mu_1 + j\omega\mu_2$, where μ_1 = 1,000 kPa and μ_2 = 3 Pa·s. Instantaneous values at $t = 0$ are solid, absolute values (amplitudes) are dashed. The normalized strain has units of reciprocal meters.

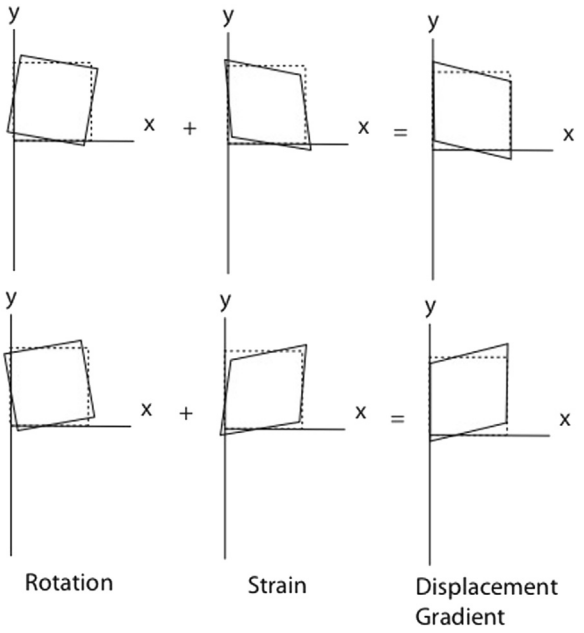

Fig. 3. Tissue distortion expressed in eqns (5)–(7). The infinite plane source at $x = 0$, coming out of the page, oscillates up (upper) and down (lower) along the y-axis. An infinitesimal square (dotted) near the source in the cross-section is simultaneously rotated and strained into a diamond shape. The rotation and strain have the same amplitudes and are directed so that their sum brings left face of the strained element back in line with the source, giving us a parallelepiped for the total distortion of the element.

magnitude to the strain (Fig. 3). The sum of strain and rotation, the displacement gradient, is a parallelepiped with its sides aligned with the wavefronts.

Rotation of a vector field is sometimes defined as equal to one-half of the curl of the vector (Graff 1975). Of course, rotation is a second-order tensor. It is the anti-symmetric part of the gradient of the displacement whereas the curl is a vector. The vector curl along with the right-hand rule is perpendicular to the plane of rotation, and its magnitude and sign tell us the direction and magnitude of the rotation. It is a specialized and very useful visual tool. Although it has no physical presence, it may be easier to visualize the physical rotation with this vector than by direct use of the rotation tensor—particularly if the coordinate system is chosen arbitrarily.

The transverse shear strain described in eqn (5) comes from off-diagonal elements of the matrix. The diagonal element in eqn (2) describes the longitudinal strain. With the hypothetical infinite piston source, the longitudinal strain is entirely compression and dilatation of the medium. The fast wave propagation constant k is orders of magnitude smaller than the slow wave constant h. There is no shear strain or rotation, and the bulk strain is very small. With more realistic, finite sources, we can have large longitudinal shear strains, but the bulk strain remains small as the examples below illustrate.

As the model systems that follow illustrate, we can have both compressional and shear longitudinal strains. The diagonal elements of the strain give us the longitudinal strains, and the off-diagonal elements, the transverse strains. The displacement gradient is the complete description of interparticle relationships. By subtracting its rotation, we are left with the strain, which is the change in shape (shear strain) and volume (bulk strain) of elements of the medium.

FIELDS OF VIBRATION SOURCES: BUBBLES

Pure plane waves are a useful idealization. They allow us to conceptualize pure, compressional, longitudinal waves and pure, shear, transverse waves. Spherical waves, however, are a practical reality. In fact, the longitudinal shear strains near bubbles in tissue are perhaps the primary concern with respect to safety in the use of diagnostic ultrasound (Carstensen et al. 2011). Furthermore, bubble fields, which involve only fast (~1,500 m/s) longitudinal waves, make a useful conceptual transition from idealized plane waves to more realistic low-frequency waves, which, in general, involve both fast and slow longitudinal and transverse waves.

Gas bodies that resonate in the megahertz frequency range—in particular, gas bodies in blood—are very nearly spherical, and almost all models of cavitation start with that assumption. At low frequencies, resonant gas bodies in tissues are rarely perfectly spherical. However, treating them as such in studying their biological effects can provide useful, semiquantitative approximations (Carstensen et al. 2011).

The displacement field of a radially oscillating sphere is given by

$$\vec{\xi}(r) = \xi_0 e^{j(\omega t - k(r-a))} \frac{a^2}{r^2} \frac{(1+jkr)}{(1+jka)} \vec{e}_r \qquad (8)$$

where ξ_0 is the displacement amplitude of the source sphere, a is the radius of the sphere, r is the point of observation relative to the center of the sphere, $\kappa = \omega/c_f$ as defined above and $\vec{e}_r$ is the unit vector in the radial direction (Carstensen et al. 2011; Graff 1975). Waves produced in the medium are irrotational and longitudinal throughout; that is, displacements are in the direction of propagation. In this case, longitudinal and radial are synonymous.

At the low frequencies that are of interest in this discussion, the products $ka < kr << 1$, and at low

frequencies, we can treat both c_f and k as real numbers. The gradient of the displacement is

$$\nabla \vec{\xi}\,(r,t) = \overrightarrow{\overrightarrow{S}} = \xi_0 e^{j(\omega t - k(r-a))} \frac{a^2}{r^3} \frac{1+jkr}{1+jka} \begin{bmatrix} -2+\dfrac{k^2r^2}{1+jkr} & 0 & 0 \\ 0 & 1 & 0 \\ 0 & 0 & 1 \end{bmatrix} \tag{9}$$

and because there is no rotation, the displacement gradient is also the strain. Equation (9) differs qualitatively from eqn (2), the gradient for longitudinal plane waves. Despite the fact that the displacement is only in the radial direction, we now have lateral strain. It arises from the fact that as elemental cubes of the medium move out radially, they become thin, rectangular parallelepipeds. This occurs even if the medium is incompressible ($k = 0$). Equivoluminal shape change is shear strain. In contrast to plane waves, the longitudinal shear strain that we find in spherical coordinates arises from the axial thinning that occurs as a fixed volume of the medium moves outward radially. The fixed volume of an element of the medium means that the magnitude of the radial thinning is twice the polar and the azimuthal stretching. In the present case, the shear strain is

$$\overrightarrow{\overrightarrow{S}}_s = \xi_0 e^{j(\omega t - k(r-a))} \frac{a^2}{r^3} \frac{1+jkr}{1+jka} \begin{bmatrix} -2 & 0 & 0 \\ 0 & 1 & 0 \\ 0 & 0 & 1 \end{bmatrix} \tag{10}$$

and the bulk strain is

$$\overrightarrow{\overrightarrow{S}}_b = \xi_0 e^{j(\omega t - k(r-a))} \frac{a^2}{r^3} \frac{1+jkr}{1+jka} \begin{bmatrix} \dfrac{k^2r^2}{1+jkr} & 0 & 0 \\ 0 & 0 & 0 \\ 0 & 0 & 0 \end{bmatrix} \tag{11}$$

The interesting difference between longitudinal plane wave and the longitudinal spherical wave is that we now have both compressional and shear waves and the shear strains are much greater than the bulk strains (Fig. 4). In Figures 4–6, we can see the transition from characteristically spherical wave behavior to plane wave behavior as distance from the source, frequency and size of the source increase. Figure 4 illustrates the strains near an oscillating bubble in a representative tissue for a low frequency of interest here. The particle displacements are entirely radial (longitudinal). The shear strain, characterized by S_{rr}–$\Delta V/V$, $S_{\theta\theta}$ and $S_{\phi\phi}$ is entirely longitudinal and irrotational. Note that the bulk strain is roughly three orders of magnitude smaller than the shear strain near the sphere. The shear strain has a stronger dependence on r than the bulk strain. But, they do not become comparable in magnitude within a distance of 10 cm in this example.

Figure 5 illustrates that the shear strain is roughly independent of frequency. At frequencies where $kr < 1$, the bulk strain is directly proportional to frequency squared. Therefore, shear strain shifts from dominance of the propagated waves by shear strains at low frequency to dominance by bulk strain at high frequency. In this example, the transition takes place at $\omega \sim 10^5$/s or ~20 kHz. Beyond that point, S_{rr} and bulk strain increase with first power of frequency. At low frequencies, thinning of an element of the medium in the radial direction is nearly compensated by expansion in the two transverse directions—very small change in volume. At high frequencies, radial thinning is no longer completely compensated by transverse expansion, leading to dominance by bulk strain. We see in Figure 5 how it is possible at megahertz frequencies to assume that tissue is a fluid. Stress and bulk strain at those frequencies are related by a single constant and it is possible to treat both as simple scalars.

Figure 6 illustrates the transformation from shear to bulk dominance as the size of the source increases. The strains are shown for a position 1 cm from the surface

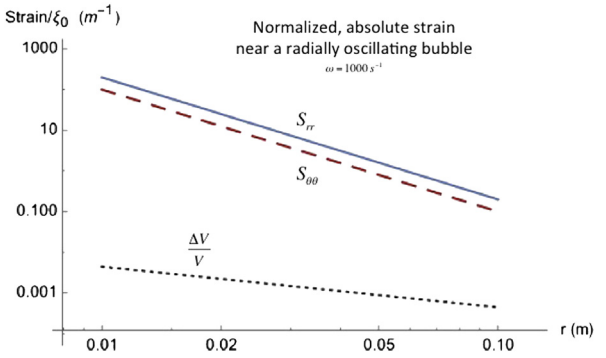

Fig. 4. Normalized, absolute strain near a radially oscillating bubble S_{rr} (solid), $S_{\theta\theta} = S_{\varphi\varphi}$ (dashed), $\Delta V/V$ (dotted). a = 0.01 m, ω = 1,000/s, ρ = 1,000 kg/m^3, c_f = 1,500 m/s.

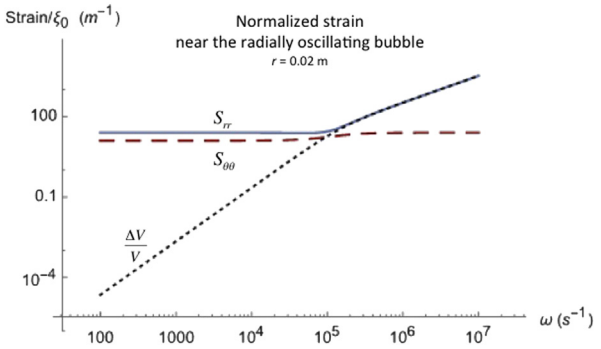

Fig. 5. Normalized strain near the radially oscillating bubble of Figure 4, r = 0.02 m. All other parameters are the same as in Figure 4.

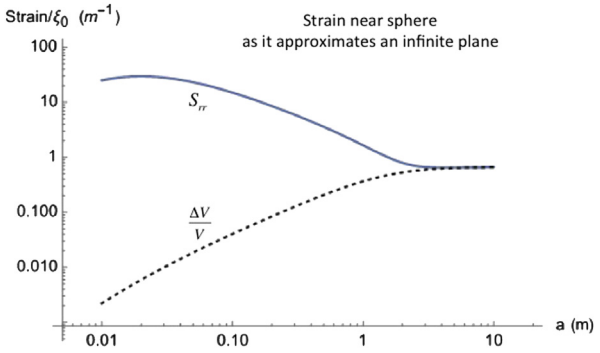

Fig. 6. Normalized strain near a radially oscillating bubble as it approximates an infinite plane. $r = a + 0.01$ m. All other parameters are the same as in Figure 4.

of the sphere as the size of the sphere increases. At ω = 1,000/s (~150 Hz), the radius of curvature of the source must be greater than 1 m (approximately one wavelength) before we reach the "plane wave" case.

For the radially oscillating sphere, there are no slow waves. Both shear and bulk strains are longitudinal and propagate at velocities on the order of 1,500 m/s.

For elastographers, fast waves of the kind generated by spherically oscillating sources contain no useful information and are a potential source of error (Carstensen and Parker 2015). However, there are many examples of biological effects from bubble sources, indicating that shear strains from fast waves can produce bio-effects if their amplitude is sufficiently high.

In summary, as the spherical source expands, it displaces the medium adjacent to it and, in the process, causes two strains in this region: (i) longitudinal shear strain and (ii) bulk strain. Remember that the displacements in this example are purely radial. So, the shear strain occurs simply because the polar dimension of an element increases when the radial position increases.

FIELDS OF VIBRATION SOURCES: ACOUSTIC DIPOLE

Now take two spherical sources each with amplitude ξ_0 like those just discussed, place them a distance d apart, and let one of them contract while the other is expanding. Let the origin of our spherical coordinate system be the midpoint between the two sources. Furthermore, let the separation d be small, and call the product $\xi_0 d$ the dipole moment. Let the point of observation r be large compared with d. Adding two appropriately phased fields of the form of eqn (8), we have, after some arithmetic (Chanaud 2010),

$$\vec{\xi}(r,\theta,t) \sim \xi_0 d \frac{e^{j(\omega t - kr)}}{r^3}\left\{(2+2jkr-k^2r^2)\cos\theta\vec{e}_r+(1+jkr)\sin\theta\vec{e}_\theta\right\} \tag{12}$$

At low frequencies, deleting terms for which $d/r < 1$ results in errors of a few parts per million from the complete solution.

Equation (12) indicates that as we add two fast longitudinal waves with opposing phases, the resulting field has fast transverse as well as fast longitudinal displacements. The transverse wave has its maximum amplitude at $\theta = \pi/2$.

The gradient of the displacement in this case is also the strain:

$$\nabla\vec{\xi}(r,\theta,t) = \overrightarrow{\overrightarrow{S}} \sim \xi_0 d \frac{e^{j(\omega t - kr)}}{r^4}\begin{bmatrix} (-6-6jkr+3k^2r^2+jk^3r^3)\cos\theta & -(3+3jkr-k^2r^2)\sin\theta & 0 \\ -(3+3jkr-k^2r^2)\sin\theta & (3+3jkr-k^2r^2)\cos\theta & 0 \\ 0 & 0 & (3+3jkr-k^2r^2)\cos\theta \end{bmatrix} \tag{13}$$

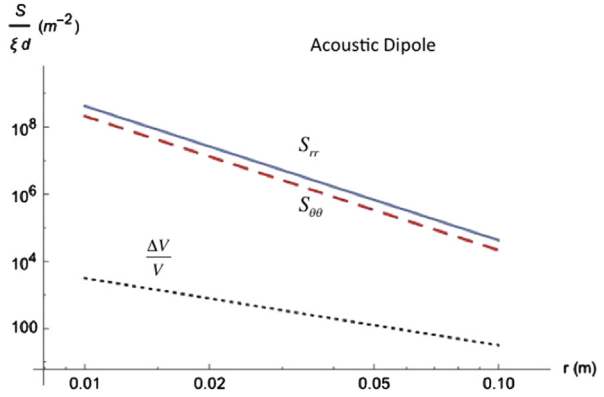

Fig. 7. Normalized, absolute strain near an acoustic dipole. S_{rr} (*solid*), $S_{\theta\theta} = S_{\phi\phi}$ (*dashed*), $\Delta V/V$ (*dotted*). ω = 1,000/s, ρ = 1,000 kg/m^3, c_f = 1,500 m/s, $\theta = 0$.

Comparing eqn (13) with eqn (9), we now have off-diagonal, transverse elements in the gradient tensor and strain. They are equal, telling us that there is no rotation—not surprising in view of the fact that we have simply added two irrotational fields. But, we have both transverse and longitudinal strain. As illustrated in Figure 7, that strain is almost entirely shear. Not shown in the figure are the off-diagonal elements, which are zero at $\theta = 0$ but are equal in magnitude to the dashed curve at $\theta = \pi/2$. The diagonal elements of eqn (13) would sum to zero (longitudinal shear strain) were it not for the term in k^3r^3 (bulk strain). Just as in eqn (9), this gives the bulk strain a $1/r$ dependence when $kr > 1$.

Summarizing up to this point, the strains near small sources at low frequency are largely shear. Combinations of purely longitudinal waves can produce sums that include transverse displacements and transverse strains. The bulk strain of an acoustic dipole, which is small throughout the medium, goes to zero at $\theta = \pi/2$. Along that axis, square elements of the medium become diamond shaped without rotating, their diagonals alternatively stretching and contracting as the wave passes.

FIELDS OF VIBRATION SOURCES: TRANSLATING SPHERE

In general at low frequencies, vibration sources produce both fast and slow waves, and each can have longitudinal and transverse shear strains. Perhaps the simplest source that illustrates these general properties is a rigid sphere oscillating in translation.

Several branches of elastography obtain all the information they need from observations of particle displacements. Finding wave speed and spatial variations in amplitude from displacements makes it possible to compute diagnostically relevant elastic properties of tissue, bypassing a need to know directly what strains the tissues undergo. For low-frequency bio-effects, in contrast, it is the gradient of the displacement, rather than the displacement itself, that tells us, at the most basic physical level, what is happening to the tissue.

Imagine a small sphere embedded in a soft tissue, such as liver. As the sphere moves back and forth, it generates shear strain in the medium around it and, in that sense, it serves as a surrogate for most sources of shear strain that are of biological interest. Fortunately, we have a rigorous, analytical treatment of that phenomenon for the case of a sphere in a simple viscoelastic medium (Oestreicher 1951). It provides a detailed picture of the complex interactions that occur with movement of the sphere in such a medium. This discussion concentrates on the resulting shear strains that are the cause of biological effects. An evaluation of the displacement fields for the translating sphere is presented in Carstensen and Parker (2015).

In spherical coordinates,

$$\vec{\xi}(r,\theta,t) = \xi_0 e^{j\omega t}\left(\xi_r(r)\cos\theta\vec{e_r} + \xi_0(r)\sin\theta\vec{e_\theta}\right) \quad (14)$$

where

$$\xi_r(r) = \frac{a^3}{r^3}\left(\frac{e^{-jk(r-a)}\left(3+3jha-(ha)^2\right)\left(-2-j2kr+(kr)^2\right)}{\left(2+2jka-(ka)^2\right)(ha)^2+(ka)^2(1+jha)} + \frac{e^{-jh(r-a)}2\left(3+3jka-(ka)^2\right)(1+jhr)}{\left(2+2jka-(ka)^2\right)(ha)^2+(ka)^2(1+jha)}\right) \quad (15)$$

$$\xi_\theta(r) = -\frac{a^3}{r^3}\left(\frac{e^{-jk(r-a)}\left(3+3jha-(ha)^2\right)(1+jkr)}{\left(2+2jka-(ka)^2\right)(ha)^2+(ka)^2(1+jha)} - \frac{e^{-jh(r-a)}\left(3+3jka-(ka)^2\right)\left(1+jhr-(hr)^2\right)}{\left(2+2jka-(ka)^2\right)(ha)^2+(ka)^2(1+jha)}\right) \quad (16)$$

From this, it is clear that (i) the waves propagate radially; (ii) longitudinal displacement is proportional to cos θ and transverse displacement is proportional to sin θ; (iii) each component has a fast wave and a slow wave contribution; (iv) in many cases, effects are confined to a small region near the source of vibration, as indicated by the inverse third power of the radial variable; (v) magnitudes of fast and slow wave amplitudes are comparable in many cases; (vi) wavelengths of the fast waves are large compared with the size of exposed regions, hence these waves have a constant phase relationship to the source throughout any reasonably sized region of tissue; (vii) wavelengths of the slow waves are on the order of centimeters and thus, as radial position increases, have a cyclic phase relationship with the source and the fast waves; (viii) net displacements are in the direction of the axis of oscillation of the sphere at its surface and tend toward that direction throughout the surrounding medium; and (ix) displacements are longitudinal at $\theta = 0$ and $\theta = \pi$ and transverse at $\theta = \pi/2$ but, in general, are combinations of the two.

With bio-effects as our target subject, we need here to look carefully at what actually takes place in the simple viscoelastic medium that serves as our description of tissue. As the sphere moves forward and backward, it displaces elements of the surrounding medium. These elements, in turn, displace others more distant, and waves of displacement propagate into the medium. The speeds at which these displacements propagate depend on the stiffness of the media.

Computational tools make it straightforward to obtain analytical expressions and specific numerical examples for the gradient of the displacement, the strain and the rotation from Oestreicher's full solution of the translating sphere problem. The gradient of the displacement is

$$\nabla \vec{\xi} = \begin{bmatrix} S_{rr} & S_{r\theta}+R & 0 \\ S_{r\theta}-R & S_{\theta\theta} & 0 \\ 0 & 0 & S_{\phi\phi} \end{bmatrix} \qquad (17)$$

The upper row of the gradient of the vector displacement (eqn 17) contains the components of the gradient of the scalar, radial component of the displacement; the second row, the polar component; and so on. Along the axis of oscillation of the source sphere, there is no displacement of the medium in the azimuthal direction; simply moving the sphere stretches an element in the azimuthal direction—very much like the two illustrations for spherical waves above (Figs. 4 and 7). In fact, the strains in the polar and azimuthal directions are equal. Hence, we have a non-zero value for $S_{\phi\phi}$ even though the displacement is independent of ϕ. The symmetric part of this tensor is the strain, and the anti-symmetric part is the rotation. The sum of the diagonal elements of the tensor, its trace, is the scalar, relative change of volume of the medium. The strain itself can be written as the sum of the bulk strain and the shear strain, as in eqns (11) and (12).

For any low-frequency stresses we experience in the real world, the tissue response is almost entirely shear strain, not bulk strain or compression. The term *compression* is frequently used rather loosely in the bio-effects literature and even in some aspects of elastography. However, whether stresses are longitudinal or transverse or waves fast or slow, the low-frequency bulk strains (compression and dilatation) of the tissue are many orders of magnitude smaller than the shear strains (Fig. 8). For soft tissues in the frequency range of interest in this review, Poisson's ratio differs from 0.5 by less than one part in a million. That is to say, in most strain estimates, tissue is effectively incompressible, but shape is readily changed.

Figures 8–10, prepared with the full Oestreicher solution, give quantitative perspective to the elements of eqn (17). Figure 8 is a quantitative illustration wherein a sphere of 1-cm radius oscillates along the $\theta = 0$ axis. Parameters have been chosen to be representative of soft tissues($\mu_1 = 3$ kPa, $\mu_1 = 3$ Pa s). By observing along the radial parameter at $\theta = \pi/4$, the radial and polar contributions to the strains are given equal weight. Near the sphere, the bulk strain is smaller than the transverse and longitudinal shear strains by approximately five orders of magnitude. The small values for the ratio of bulk to shear strains in Figure 8 are similar to those for the "bubble" in Figure 4 and for the dipole in Figure 7. However, there is no transverse strain from the bubble, and neither the bubble nor the dipole has slow wave fields.

Figure 9, like Figure 5 for the bubble, illustrates that the dominance of shear strain is a low-frequency

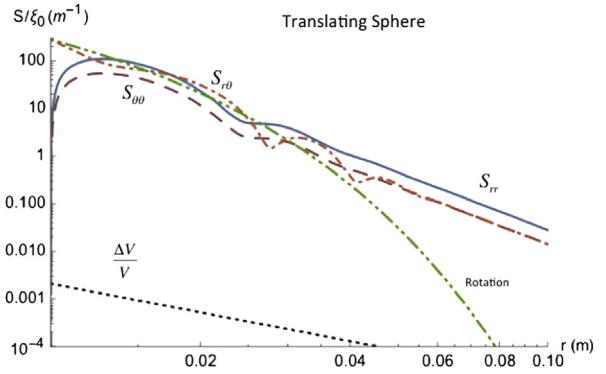

Fig. 8. Normalized, absolute strain near a transversely oscillating sphere. S_{rr} (*solid*), $S_{\theta\theta} = S_{\varphi\varphi}$ (*dashed*), $\Delta V/V$ (*dotted*), $S_{r\theta}$(*dot-dash*), R (*double dot-dash*). $a = 0.01$ m, $\omega = 1{,}000$/s, $c_f = 1{,}500$ m/s, $\mu_1 = 3$ kPa, $\mu_2 = 3$ Pa·s, $\rho = 1{,}000$ kg/m^3, $\theta = \pi/4$.

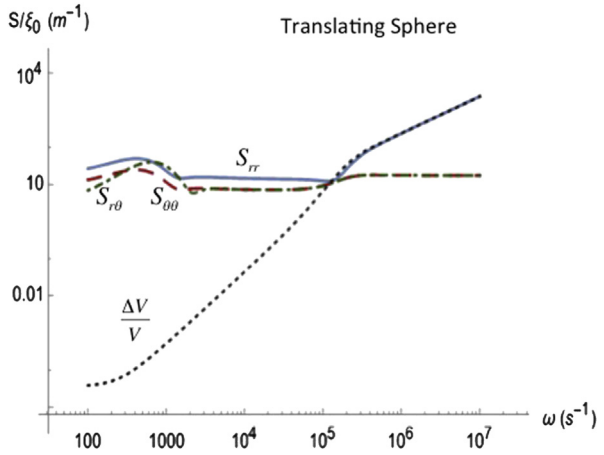

Fig. 9. Normalized, absolute strain near a transversely oscillating sphere. S_{rr} (solid), $S_{\theta\theta} = S_{\varphi\varphi}$ (*dashed*), $\Delta V/V$(*dotted*), $S_{r\theta}$(*dot-dash*ed). $a = 0.01$ m, $r = 0.02$ m, $c_f = 1{,}500$ m/s, $\mu_1 = 3$ kPa, $\mu_2 = 3$ Pa·s, $\rho = 1{,}000$ kg/m^3, $\theta = \pi/4$.

phenomenon. Above an angular frequency of about 10^5/s (~20 kHz), bulk strain (resulting from compression in the radial direction) takes over and dominates wave propagation. We see in this way how it has been possible to model wave propagation in diagnostic ultrasound as though acoustic pressure and strains of the tissue were simple scalars, while the actual tensor properties of these fields must be considered at low frequencies. Compression, of course, comes from the longitudinal strains and occurs because the lateral expansion fails to completely compensate for the radial contraction.

Figure 10, like Figure 6 for the bubble source, illustrates the transition from dominance of the strain near the sphere from shear to bulk as the size of the source increases and the driving surface approaches a plane (eqn 2). Of course, for bulk strain to be a significant factor, the source would be much larger than any region of

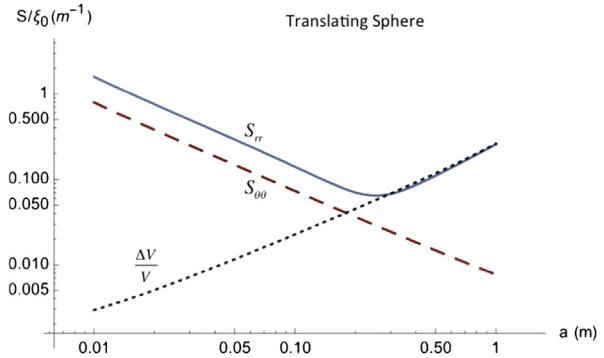

Fig. 10. Normalized, absolute strain near a transversely oscillating sphere. S_{rr} (solid), $S_{\theta\theta} = S_{\varphi\varphi}$ (*dashed*), $\Delta V/V$ (*dotted*). $r = a + 10$ μm, $c_f = 1{,}500$ m/s, $\mu_1 = 3$ kPa, $\mu_2 = 3$ Pa·s, $\rho = 1{,}000$ kg/m^3, $\theta = 0$.

interest in the human body. The bottom line from Figures 2–10 is that near realistic sources at low frequency, the strains are almost entirely shear.

In fact, we can greatly simplify expressions for the elements of the displacement and still have useful accuracy by assuming that $k = 0$. In addition, assume that $ha > 1$, which is frequently valid. With those simplifications, the elements of the displacement gradient in eqn (17) become

$$S_{rr} \sim -3\xi_0 e^{j\omega t}\cos\theta\left(\frac{a^3}{r^4} - \frac{a}{r^2}e^{-jh(r-a)}\right) \sim -2S_{\theta\theta} = -2S_{\phi\phi} \tag{18}$$

$$S_{r\theta} \sim -\frac{3\xi_0 e^{j\omega t}\sin\theta}{r}\left(2\frac{a^3}{r^4} - \frac{jha}{r}e^{-jh(r-a)}\right) \tag{19}$$

and

$$R \sim -\frac{3\xi_0 e^{j\omega t}\sin\theta}{4}\left(\frac{jha}{r}e^{-jh(r-a)}\right) \tag{20}$$

These approximations have sacrificed the information that the full equations give us on the bulk strain, but still give good approximations for the magnitude and phase of the elements of the displacement tensor otherwise. The first terms in eqns (18) and (19) are the contributions of the fast wave to the strain. Even though these equations assume that the medium is incompressible (bulk strain is negligibly small), the contribution of the fast wave to the shear strains is of the same order of magnitude as that of the slow wave.

The longitudinal strains S_{rr}, $S_{\theta\theta}$ and $S_{\varphi\varphi}$ are proportional to $\cos\theta$, and the transverse strain $S_{r\theta}$ is proportional to $\sin\theta$. Hence we can think of the displacement gradient (eqn 17) and the strain as being purely diagonal at $\theta = 0$. Then as we move around the sphere to $\theta = \pi/2$, the diagonal elements fade away, and the transverse off-diagonal elements gradually appear and finally completely dominate the matrix.

Despite the obvious differences between the strain fields of bubble sources and translating spheres, their fields have general similarities as illustrated by comparison of Figures 8–10 with Figures 4–6. The normalized magnitudes of the strains are comparable in the two cases. The frequencies at which bulk strain begins to dominate the total strain are similar. Transition from shear to compression as the source becomes larger is much the same for the two sources. Longitudinal and transverse strains differ qualitatively and, therefore, may have different biological effects. But, whether longitudinal or transverse, the fast and slow strains are physically the same. They differ only in spatial frequency.

At low frequencies, wavelengths for the fast waves are very large compared with the size of organs in the human body, and thus, the phase of the fast wave is the same throughout its field. The slow wavelengths are on the order of a centimeter. Near the sphere, the magnitudes of the two waves are comparable, and they add to and subtract from each other. It is as though we have a standing wave in which both contributions propagate in the same direction.

Because of viscous losses, the slow waves are rapidly attenuated, and fast waves dominate the shear fields beyond a few centimeters from the sphere surface. Multiplying the displacement gradient by a small position vector tells us how the displacement changes between those two points. Using that property of the gradient allows us to view the shape changes in the elements that make up the medium. Figure 11, although more illustrative than quantitative, is based on those computations.

Along the axis of oscillation, we can think of an element of the medium as a constant-volume section of a narrow cone that has its apex at the center of the coordinate system. As the element is pushed outward by the movement of the sphere, it becomes thinner and wider. The reverse takes place along the $\theta = \pi$ axis. This is equivalent to saying that an elemental sphere becomes an oblate ellipsoid in front of the sphere, whereas a spherical element at the rear ($\theta = \pi$) becomes a prolate ellipsoid. Longitudinal strain has the same physical effect on the medium whether it is generated by fast or by slow waves. All bulk strain is irrotational.

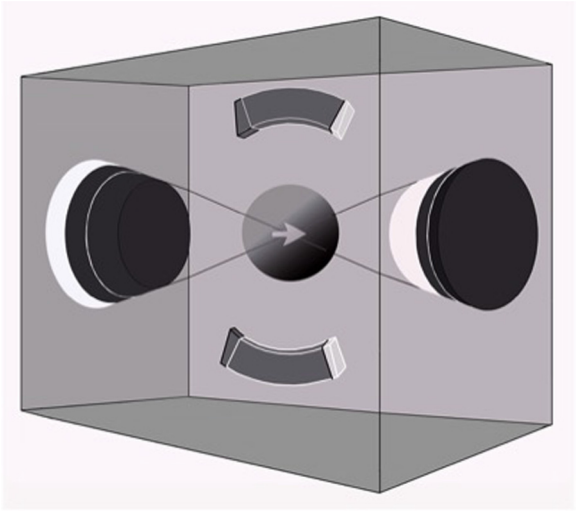

Fig. 11. Original elements (*white*) of tissue about 1 cm from the surface of a 1-cm sphere undergo shear strain (*black*); that is, they change shape without change in volume, as the sphere moves forward. The longitudinal strain along the axis of oscillation is actually three dimensional; that is, as the axial dimension of the element changes, both orthogonal dimensions change, keeping the volume constant. At $\theta = \pi/2$, shear is two dimensional; that is, there are no azimuthal contributions to the shear strain along $\vec{e_\phi}$ at $\theta = \pi/2$. Parameters used in the computations are the same as those in Figures 7–9.

Transverse shear waves differ qualitatively from longitudinal waves. Transverse waves are two dimensional; that is, there is no distortion in the azimuthal dimension. In addition, slow transverse waves rotate the medium as well as produce shear strain. At $\theta = \pi/2$, where the motion of the medium is entirely transverse, Figure 11 illustrates that even as close as 1 cm from the surface of the sphere, the direction of shear is opposite that which occurs at the surface.

Figure 12 illustrates the effects of source translation on fast and slow shear at $\theta = \pi/2$, 2 mm from a 1-cm sphere with an amplitude $\xi_0 = 1$ mm. At $\theta = \pi/2$, the particle displacements are all in the θ direction, but the space rate of change in the r direction has its maximum at $\theta = \pi/2$. Hence much of the strain comes from change in the θ displacement with change in r.

Because strain concerns interparticle relationships, we pick a particle and draw an infinitesimal square about it large enough that it contains several other particles. The figure illustrates the extremes (*solid and dotted*) in shape change attributable to the fast and slow waves. We postulate that for bio-effects, tissue cares little about its phase relative to the source. But, when we add the effects of fast and slow waves on the shape of the square, we must take their relative phases into account. The total strain may be the fundamental physical correlate for bio-effects, but it does not completely describe what happens to the square as it is being strained. The slow wave simultaneously rotates the element so that the bottom boundary remains approximately parallel to the surface of the sphere.

SHEAR STRAIN AND BIO-EFFECTS

Tissues exposed to low-frequency vibration experience shear strains. Those strains must be the primary physical phenomena that lead to biological effects. The discussion thus far, which has considered both transverse and longitudinal plane waves and spherical waves generated by radially and transversely oscillating spheres, provides us with examples of the kinds of shear strains that are produced by realistic sources of vibration. These analytical examples tell us the kinds of physical distortions we can expect in specific applications.

Numerical methods could be used to determine the actual strains in any specific application, or strains might be measured directly using techniques that have been developed in the field of elastography. To put that in perspective, consider the demands of bio-effects research at megahertz frequencies. Reporting the pressure fields to which biological samples are exposed is a minimum requirement for publication. As Figure 9 illustrates,

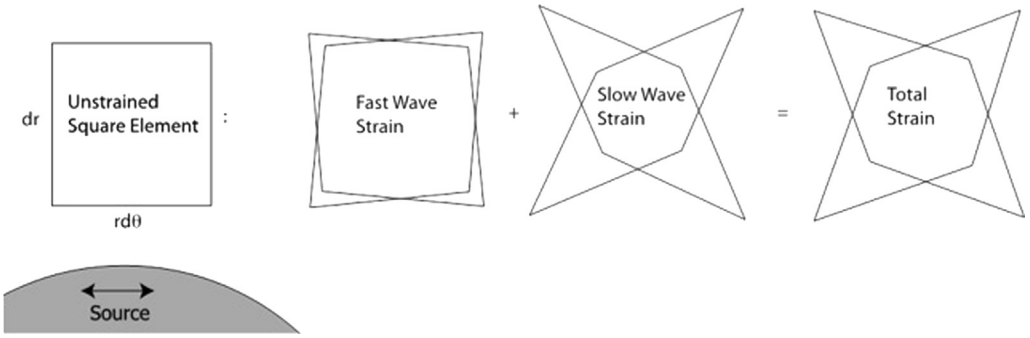

Fig. 12. Strains attributable to fast and slow waves 2 mm from the surface of a 1-cm sphere moving right and left with an amplitude of 1 mm. *Solid and dotted parallelograms* indicate the extremes of distortion of a square element of the medium. c_f = 1,500 m/s, c_s = 1.7 m/s, that is, μ_1 = 3 kPa, μ_2 = 0, ρ = 1,000 kg/m^3, ω = 1,000/s (∼160 Hz), $\theta = \pi/2$, ξ_0 = 1 mm.

bulk strain dominates at those frequencies, and going from acoustic pressure to strain is the simple ratio of two "scalars": pressure and bulk modulus. So, requiring knowledge of pressure in a high-frequency study is equivalent to requiring a value of the bulk strain that was produced. Applying the same standard to low frequency bio-effects research means that a minimum requirement for publication would be a quantitative value for shear strain, a second-order tensor. Thus, the challenge may be somewhat greater for today's low-frequency bio-effects investigator, but in view of the fundamental role of shear strain, attempts to quantify and report shear strain of tissues during the analysis of vibration-mediated bio-effects is a reasonable and critical objective for advancing bio-effects research and establishing appropriate exposure guidelines.

TACTILE PERCEPTION

A few examples from the literature on tactile perception serve to illustrate how quantification of tissue shear strain is key to understanding the biological response to vibration. Many of the cells in our bodies are exquisitely sensitive to shear strains. A century and more of research on the phenomenon has produced a rich understanding of the neurological processes involved, and we cite it briefly here only to emphasize that shear strain is the key physical parameter in every neural response to purely mechanical stimuli. Regardless of the stresses that produce the strain, it is the shear strain and its time rate of change that are directly related to the biological effect of perception.

Before even considering the neurologic aspects of perception, Oestreicher's theory has some interesting information for us about the strain itself. Referring back to Figure 8, note that the net surface longitudinal strain is zero. The fast and slow waves are of equal amplitude and out of phase at the surface. The net longitudinal strain becomes finite a millimeter or two from the surface. Frequency has little effect on this phenomenon.

In contrast, the net surface transverse strain (Fig. 8) is finite and large. So, the greater sensitivity of the finger to stroking a surface as opposed to simply contacting it may, in part, be mechanical. The details are contained in eqns (18) and (19). The magnitude of the transverse, surface strain, normalized by the amplitude of oscillation of the sphere, is roughly independent of frequency. An experimental study of transverse and longitudinal strains is discussed below.

Scientists have identified several different families of mechanosensitive ion channels, structures in the nerves that open in response to tissue deformation (shear strain) and allow sodium and potassium to pass through a neuron's plasma membrane, leading to the generation of nerve impulses. There are four main types of mechanosensitive afferent nerves in hairless human skin: Pacinian (or Lamellar) corpuscles, Meissner's corpuscles, Merkel's discs and Ruffini endings.

Pacinian corpuscles play a role in our sense of touch and are especially sensitive to vibratory stimuli in the frequency range 40–1,000 Hz, producing their maximum response when the strain changes at frequencies of around 250 Hz (Bell et al. 1994; Scheibert et al. 2009). Of the four major types of mechanosensitive neurons, Pacinian corpuscles are the most sensitive, with tissue deformation of as little as 10 nm giving rise to an action potential (Bell et al. 1994). Pacinian corpuscles are located at the base of the dermis, which places them 2 or 3 mm from the surface of the skin. As illustrated in Figure 13, that depth is great enough that Pacinians experience significant longitudinal as well as transverse strains from surface excitation.

In light of the preceding discussion, a study by Brisben et al. (1999) is of particular interest in several respects. Brisben and colleagues' subjects grasped a cylinder whose axial displacement was monitored as

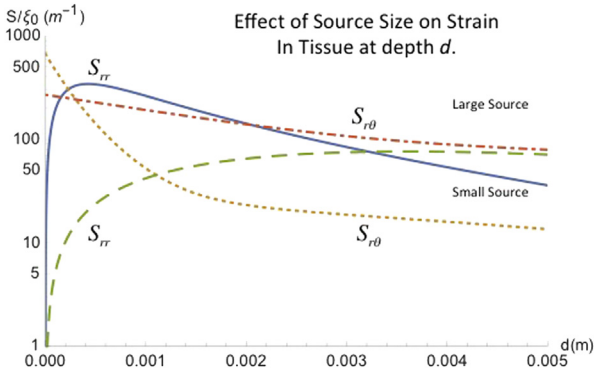

Fig. 13. Use of Oestreicher's model of an oscillating sphere to illustrate the effects of contact area on strain. $a = 1$ mm: longitudinal (*solid*) and transverse (*dotted*). $a = 2$ cm: longitudinal (*dashed*) and transverse (*dash-dotted*). Abscissa d is distance from the surface of the vibrating sphere. $\mu_1 = 3$ kPa, $\mu_2 = 3$ Pa·s, $\omega = 2\pi$ 160/s.

the subjects reported perceived vibration over the frequency range 10 to 300 Hz. The sensitivities observed in this study were significantly greater than accepted values at the time of the study. The maximum sensitivity for the study group as a whole was ∼20 nm at 200 Hz. One subject responded reliably at 10 nm! Oestreicher's theory, used for Figure 13, gives us an order-of-magnitude estimate of the strain magnitudes that correspond to a transverse surface displacement of 10 nm, or $\sim 2 \times 10^{-6}$ for the transverse strain and $\sim 2 \times 10^{-3}$ s^{-1} for the rate of strain. It seems that only Brownian motion limits perception. The only other report of such low thresholds known to these authors was a 1939 investigation by von Békésy, who used a transverse excitation as well (von Békésy 1939).

Brisben and co-workers carried out several exploratory experiments to learn the details of this high perceptual sensitivity. Among these tests was a comparison of the effects of stimulation parallel and perpendicular to the skin surface. They found that the threshold for perpendicular excitation was 9 dB (a factor of ∼3 in displacement amplitude) greater than that for parallel motion at 300 Hz.

Part of the difference in sensitivity with direction of excitation was because a somewhat larger area was displaced when the subjects grasped a cylinder than when a 1-mm probe was used for stimulation. To isolate that variable, the investigators compared displacements normal and parallel to the skin surface, keeping the contact area the same in each comparison. They found thresholds for normal stimulation still to be higher than those for parallel stimulation by a factor of approximately 2 whether the contact areas were either 0.01 or 1 cm^2. So, we should look first for a mechanical difference in these exposures—specifically, the strains at the presumed depth of the sensory nerves. Figure 13 (eqns 18 and 19) serves primarily to illustrate the complexity of the strain fields. In this example, the transverse strain at 3-mm depth for the small source is only about one-third the value for longitudinal strains. The subject merits further study starting with a more realistic model of the tissue.

Pacinians become less sensitive with age. To illustrate, consider Verrillo's (1980) studies of the effects of aging on thresholds for vibrotactile perception (Fig. 14). Subjects placed their right hand on a flat plate with the thenar eminence (the muscle pad at the base of the thumb) centered on a 1-cm-radius vibrator protruding 0.5 mm into the hand. The surrounding stationary plate damped wave motion in the skin lateral to the source. The 250-Hz source was pulsed 1 s on and 1 s off. Threshold source displacements amplitudes were reported. Thresholds for the younger groups in Verrillo's (1980) study are comparable to those of Brisben et al. (1999) for longitudinal excitation and roughly five times higher than those for transverse strain. The investigators tested the oldest group for possible neuropathies, but found no pathologic explanation for the rapid decrease in sensitivity beyond age 50.

BIOLOGICAL EFFECTS OF VIBRATION ON THE PERCEPTION THRESHOLD

Vibration can be an occupational hazard for construction workers. As an example of the biological effects of large low-frequency shear strains, Harada and Griffin (1991) determined the shift in perception threshold in the fingers of subjects that were exposed for 5 min

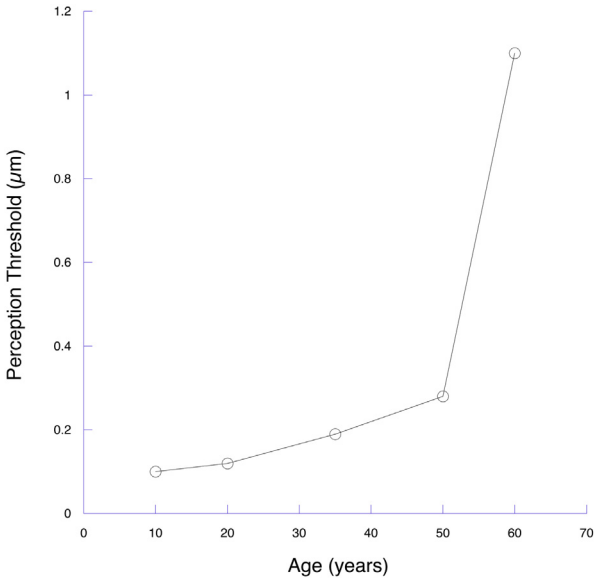

Fig. 14. Threshold for tactile perception at 250 Hz. Data from Verrillo (1980).

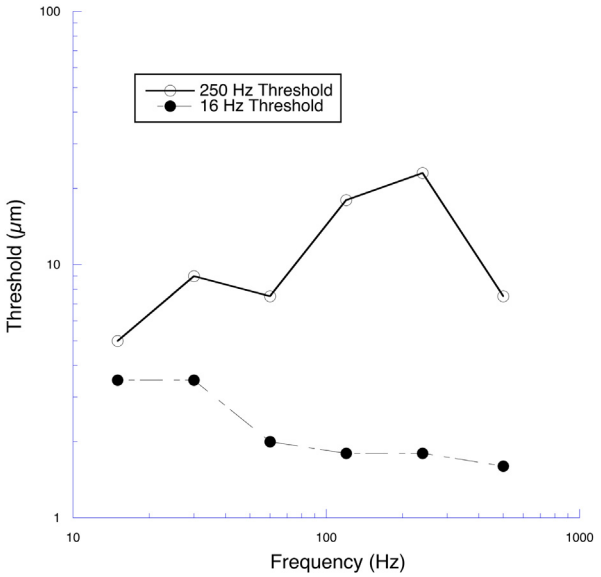

Fig. 15. Threshold shifts resulting from exposure of the hand to accelerations of 20 m/s^2. Exposures were performed over a range of frequencies. The ordinate gives the ratio of post-exposure thresholds to their normal values. The *dashed plot* is the ratio for the 250-Hz threshold, and the *solid plot* is the ratio for the 16-Hz threshold. Frequency-dependent thresholds were measured after each exposure. Adapted from Harada and Griffin (1991).

to vibration by grasping a handle that was vibrated at an acceleration of 20 m/s^2 (Fig. 15). The exposures covered the frequency range 16 to 500 Hz. Holding the acceleration constant for all exposures is equivalent to maintaining the surface force density ($\sim 2 \times 10^4$ N/m^3) the same for all exposures. The peak-to-peak amplitude for this exposure was $\sim$3 mm at 16 Hz and $\sim$10 μm at 250 Hz. In order of magnitude, this would correspond to transverse shear strains of $\sim$0.1 at the lowest frequency to 0.0001 at the highest frequency.

After exposure at 250 Hz for 5 min, the amplitude of shear strain required for detection at 250 Hz increased by more than a factor of 20. In contrast, 16-Hz exposures had their maximum effects near 16 Hz. Very likely the dominant neurons at 250 Hz were the highly sensitive Pacinian corpuscles, whereas less sensitive receptors were involved at 16 Hz. It is interesting that each receptor was most affected by exposures at its greatest sensitivity.

SUMMARY

Shear strain must be the physical basis for biological effects of low-frequency vibration—what happens physically to tissues exposed to vibration and the logical starting point for hypothesis generation in bio-effects research. With varying degrees of quantitative relevance, Oestreicher's translationally oscillating sphere illustrates the kinds of physical processes that one finds in exposed tissues. In general, we have coexisting longitudinal and transverse shear strains. Low-frequency longitudinal strains are greatest along the axis of oscillation of the source. Transverse strains are greatest when the polar angle is $\pi/2$. Bulk strains are negligibly small. Both longitudinal and transverse shear waves have slow and fast wave contributions. The effective displacements and strains from the two waves are of comparable magnitude. The strains associated with the fast wave result entirely from the very strong dependence of amplitude of the displacement on radial position. Increasing the size of the source would reduce shear strains near the source for a given source amplitude. The same can be said for the slow wave. In this case, however, both phase and magnitude dependences of displacement on radial position contribute to shear strain. In tissue, absorption increases with frequency as well and dominates slow wave strain amplitude, except at very small distances from the source.

Acknowledgments—This work is supported in part by the University of Rochester Hajim School of Engineering and Applied Sciences. The authors thank Richard Carstensen for Figure 11.

REFERENCES

Bell J, Bolanowski S, Holmes MH. The structure and function of Pacinian corpuscles: a review. Prog Neurobiol 1994;42:79–128.

Brisben AJ, Hsiao SS, Johnson KO. Detection of vibration transmitted through an object grasped in the hand. J Neurophysiol 1999;81:1548–1558.

Carstensen E, Gracewski SM, Dalecki D. Shear strain from irrotational tissue displacements near bubbles. J Acoust Soc Am 2011;130:3467–3471.

Carstensen EL, Parker KJ. Oestreicher and elastography. J Acoust Soc Am 2015;138:2317–2325.

Carstensen EL, Parker KJ. Physical models of tissue in shear fields. Ultrasound Med Biol 2014;40:655–674.

Chanaud RC. Tools for analyzing sound sources. Essex, CT: CCR Associates; 2010.

Food and Drug Administration (FDA). Diagnostic ultrasound guidance. Center for Devices and Radiological Health, FDA, U.S. Department of Health and Human Services, 1993.

Graff KF. Wave motion in elastic solids. Oxford: Clarendon Press; 1975. p. 292.

Harada N, Griffin MJ. Factors influencing vibration sense thresholds used to assess occupational exposures to hand transmitted vibration. Br J Ind Med 1991;48:185–192.

Oestreicher HL. Field and impedance of an oscillating sphere in a viscoelastic medium with an application to biophysics. J Acoust Soc Am 1951;23:704–714.

Scheibert J, Leurent S, Prevost A, Debregeas G. The role of fingerprints in the coding of tactile information probed with a biomimetic sensor. Science 2009;323:1503–1506.

Verrillo RT. Age related changes in the sensitivity to vibration. J Gerontol 1980;35:185–193.

Von Békésy G. Über die Vibrationsempfindung. Akust Z 1939;4:315–334.

APPENDIX

TERMINOLOGY

Particle displacements

The terms *longitudinal* and *transverse* describe the orientation of the particle displacements relative to the wavefront. Longitudinal displacements are in the direction of propagation. Transverse displacements are perpendicular to the direction of propagation.

Wave speed

Wave motion produced by vibrating sources may be either irrotational or incompressible. In soft tissues, irrotational wave speeds are on the order of 1,500 m/s, whereas incompressible waves range from 1 to 10 m/s. We prefer the positive descriptors, fast wave and slow wave, respectively.

Strain

Strain is the symmetric part of the displacement gradient. The anti-symmetric part is the rotation of the medium. Bulk strain is a measure of the relative change in volume (dilatation or compression) of an element of the medium. It is the divergence of the displacement, the trace of the strain or the displacement gradient tensors. Shear strain measures change in shape of an element of the medium. Depending on the direction of the particle displacements, the shear strain may be either longitudinal or transverse. We can have longitudinal shear strain and transverse shear strain. Longitudinal shear strain is three dimensional. Transverse shear strain is two dimensional.